Modelling of a deep excavation in a silty clay

Modélisation d'une excavation profonde située dans l'argile limoneuse

D. Mašín[1], J. Boháč and P. Tůma
Charles University in Prague, Czech Republic

ABSTRACT

This contribution describes numerical modelling of a deep excavation in Koper, Slovenia. The 13 m deep excavation, supported by a propped diaphragm wall, is located in Trieste bay in homogeneous deposit of marine sediments of silty clay. The excavation is located within a developed urban environment, reliable control of displacements induced by the excavation is thus required. The paper demonstrates merits of the use of advanced hypoplastic material model for soil when compared with standard Mohr-Coulomb simluations.

RÉSUMÉ

Cette contribution décrit la modélisation numérique d'une excavation profonde à Koper en Slovénie. L'excavation est profonde de 13 mètres, soutenue par un mur à diaphragme étayé. Elle se trouve dans la baie de Trieste dans les sédiments marins homogènes l'argile limoneuse. L'excavation est localisée dans un milieu urbain développé donc un contrôle fiable de déplacements provoqués par l'excavation est exigé. L'article démontre les avantages de l'utilisation d'un modèle hypoplastique plus avancé en comparaison avec les simulations standards de Mohr-Coulomb.

Keywords: soft clay, excavation, hypoplasticity, non-linearity

1 INTRODUCTION

Correct predictions of a displacement field induced by deep excavations is important especially in an urban environment. Geotechnical engineer is required to limit the movements of the adjacent buildings imposed by the excavation to an acceptable level. As demonstrated in a number of studies, correct predictions of the displacement field induced by a geotechnical structure require a soil constitutive model to be capable of correct predicting of the soil stiffness. The stiffness depends on the soil state, particularly on the current stress level and previous loading history.

In this contribution, we compare predictions of a deep excavation in soft silty clay by two constitutive models: Mohr-Coulomb model and a hypoplastic constitutive model. The predictions are compared with monitoring data. Advantages

[1] Corresponding Author.

of the use of an advanced constitutive model are demonstrated.

2 GEOLOGY OF THE KOPER HARBOUR

The excavation is located in Koper, Slovenia, at the intersection of the Kolodvorska and Ferrarska streets. SSW part of the harbour is located within a deep, partially buried valley of Rižana river. The bedrock (20-60 m deep) is formed by flysh marls. The buried valley of the Rižana is filled with sand and sandy gravel (Fig. 1).

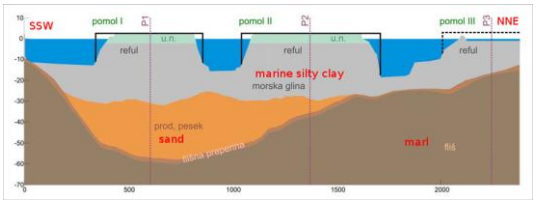

Figure 1. Geological sequence of Koper harbor (Logar 2009).

The main part of the sequence consists of Quaternary deposits of soft silty clay. Most of the geotechnical construction, including the excavation of the interest, is located in this material. It will be described in more detail in Sec. 3.

Figure 2. History of development of the Koper town and harbour, demonstrating extensive use of land reclamation (after Logar 2009).

The top part of the geological sequence is made by refilled material, composed mostly of the local marine silty clay material. It thus has similar mechanical properties as the silty clay layer below. In the town of Koper the extent of the refilled material is quite significant, as most of the harbor has been built on reclaimed land (Fig. 2).

3 PROPERTIES OF THE MARINE SILTY CLAY

The 20-30 meters thick strata of marine clay is remarkably homogeneous. This is demonstrated in Fig. 3 (Logar 2009), showing the dependence of Atterberg limits and undrained shear strength on depth.

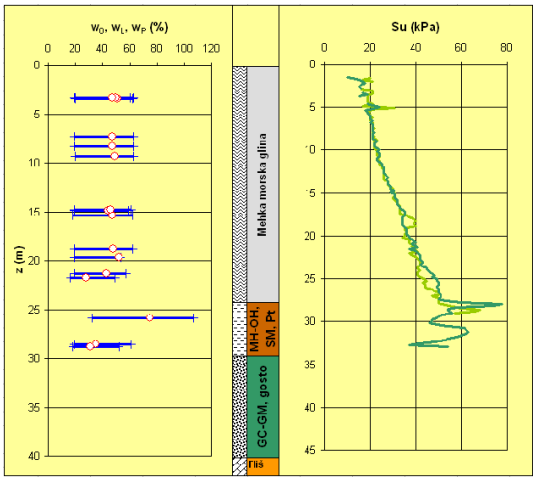

Figure 3. The dependency of Atterberg limits and undrained shear strength on depth, demonstrating homogeneity of the marine clay deposit (Logar 2009).

The samples of silty clay for the present investigation had been obtained during the excavation from a depth of 3,4 m. Altogether two cubic block samples of undisturbed clay of the size 20 x 20 x 20 cm were excavated. Thanks to the remarkable homogeneity of the clay strata, it was assumed that the soil obtained from one depth level would sufficiently represent the mechanical behavior of the whole deposit.

The material may be characterized as a grey, high plasticity carbonatic silty clay with the following index properties: w=42.6 %, w_L=64 %, w_P=34 %, I_P=30 %, ρ_s=2731 kg/m^3, carbonate content 17.6 %.

Figure 4 shows grain size distribution curve, indicating the material has 43 % of clay size particles, 45 % of silt particles and 12 % of sand particles.

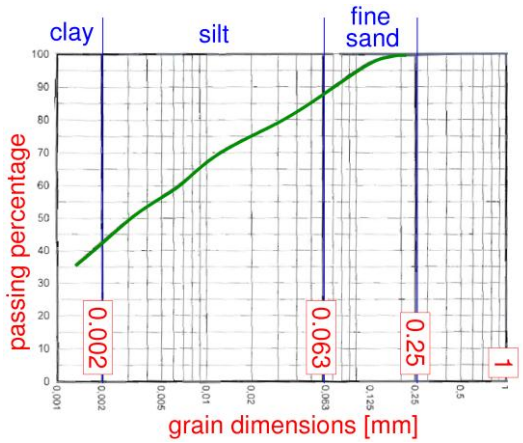

Figure 4. Grain size distribution of the silty clay used in the present investigation.

Laboratory investigation included all experiments needed to calibrate the parameters of a hypoplastic model for clays by Mašín [3]. Namely, oedometric tests on undisturbed and reconstituted material and undrained triaxial tests on undisturbed soil. The triaxial testing included instrumentation for accurate stiffness measurements in the small and very small strain range - local LVDT transducers to measure axial displacements and bender element tests to measure very small strain shear modulus using shear wave propagation velocity. Experimental data are given together with the model calibration in Sec. 5.

4 CONSTITUTIVE MODEL

Soil properties were described by means of an advanced nonlinear constitutive model for fine grained soils, a hypoplastic constitutive model for clays by Mašín [3] enhanced by the intergranular strain concept by Niemunis and Herle [4]. For comparison, the simulations were also run with the basic Mohr-Coulomb model.

The basic version of the hypoplastic model requires five parameters, whose physical interpretation corresponds to the parameters of the Modified Cam-Clay model: N, λ^*, κ^*, φ_c and r. The parameters N and λ^* define the position and the slope of the isotropic normal compression line (NCL) within the ln p vs. ln(1 + e) representation, where p is the effective mean stress and e is the void ratio. Parameter κ^* controls the slope of the isotropic unloading line. Parameter φ_c is the critical state friction angle. The parameter r controls the soil shear stiffness. In order to predict the high initial (very small strain) stiffness, its decrease with straining, and the effects of recent stress (deformation) history, the model needs to be enhanced by the intergranular strain concept [4]. The enhanced model requires additional five parameters (m_R, m_T, R, β_r and χ).

5 EXPERIMENTAL RESULTS AND MODEL CALIBRATION

The first experimental data set includes oedometer tests on reconstituted and undisturbed soil samples. Altogether, six oedometer tests were performed, three on reconstituted and three on undisturbed soil. The results are shown in Fig. 5. The initial void ratio is scattered, but the results indicate there is no apparent structuration of the natural soil:

- Normal compression lines (NCLs) of the undisturbed soil are not positioned higher in the lnσ_a (effective axial stress) vs. ln(1+e) plot than the normal compression lines of the reconstituted soil.
- NCLs of the undisturbed and reconstituted soils have the same slopes.

Thanks to the insignificant effects of structure, the structured version of hypoplastic model [2] did not have to be used and the simulations were run with the basic hypoplastic model for clays [3]. The oedometer tests were used for calibration of the material parameters λ^*=0.103, κ^*=0.015 and N=1.31 (Fig. 5).

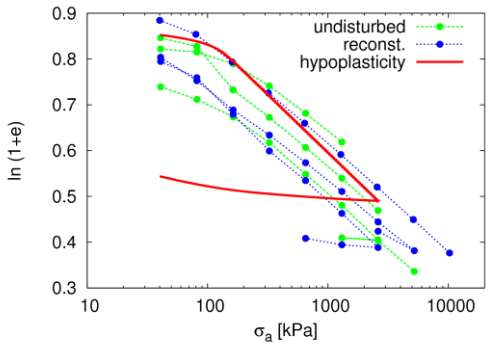

Figure 5. Results of oedometer tests on undisturbed and reconstituted soil samples, together with simulation by hypoplastic model.

In addition to the oedometer tests, three undrained triaxial tests were performed on undisturbed samples (Fig. 6). The stress paths indicate by their directions that the soil is wet side of critical. The shear tests were used for calibration of the hypoplastic parameters φ_c=33° and r=0.3 and the Mohr-Coulomb parameters φ=23°, c=15 kPa, ψ=1°, E=5 MPa and υ=0.3.

The undrained triaxial tests were performed with the equipment enabling us to study the small- to very-small strain behaviour of the soil. In particular, the small axial strains were measured using submersible LVDT strain transducers and the very-small-strain shear stiffness was measured by means of propagation of shear waves using bender elements.

Fig. 7 shows the relation between the very-small-strain shear modulus G_0 and the mean effective stress p in isotropic consolidation. The results were used for calibration of the intergranular strain concept extension of hypoplasticity. The parameter m_R influencing the dependence of G_0 on the mean stress level, was calibrated using the following equation [3]:

$$G_0 \simeq \frac{m_R}{r\lambda^*} p$$

The obtained parameters were: m_R=12, m_T=12, R=2.e-5, β_r=0.09 and χ=0.7.

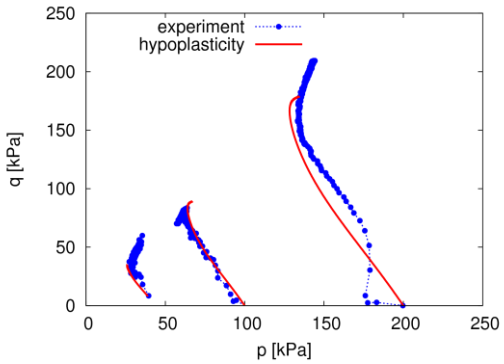

(a)

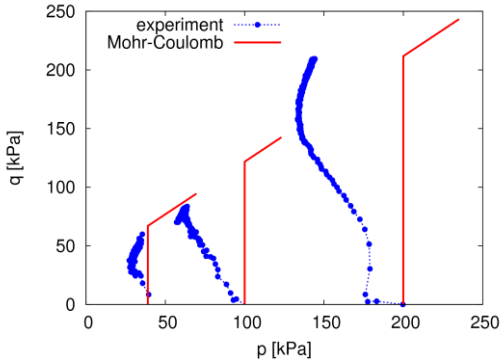

(b)

Figure 6. Stress path of undrained triaxial tests on undisturbed material and predictions by the hypoplastic and Mohr-Coulomb models.

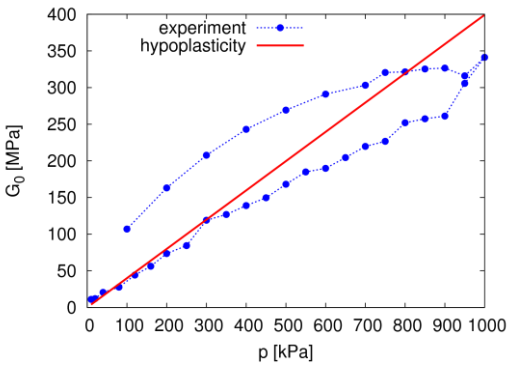

Figure 7. The dependence of the very-small-strain shear modulus on mean stress, as measured by bender elements and as predicted by the hypoplastic model.

The complete parameter sets of both hypoplastic and Mohr-Coulomb models are given in Tabs. 1. and 2.

Table 1. Parameters of the hypoplastic model

φ_c	λ^*	κ^*	N	r
33°	0.103	0.015	1.31	0.3
m_R	m_T	R	β_r	X
12	12	2.e-5	0.09	0.7

Table 2. Parameters of the Mohr-Coulomb model

φ	c	ψ	E	υ
23°	15 kPa	1°	5 MPa	0.3

6 CASE STUDY ANALYSED

The case study analysed is a 56 m long, 54 m wide and 13 m deep excavation for four-levels underground garages.

The excavation is supported by diaphragm walls, 0.8 m wide, and at least 22 m deep (depending on the position) to reach the bedrock marl. Lateral bracing was provided by five levels of permanent floor slabs. Top-down construction method was used: after reaching the required level, the excavation was stopped and the floor slab cast and connected with the diaphragm wall. The process was repeated until the final excavation depth was reached.

7 FINITE ELEMENT MODEL

The simulations have been performed using finite element software Plaxis 2D. The geometry of the problem is shown in Fig. 8.

Figure 8. Geometry of the finite element model of the excavation

All the analyses were performed as undrained. The ground water level was located 1.8 m below the surface. Void ratio was initialized such that the overconsolidation ratio (OCR) was constant with depth. Isotropic OCR, defined as a ratio of mean stress at the isotropic normal compression line and the current mean stress, was equal to 1.31. K_0 was calculated using Jáky formula $K_0 = 1 - \sin \varphi_c$ (the formula is relevant for normally consolidated soil). The bedrock marl was modelled using Mohr-Coulomb model and silty clay using both hypoplasticity and Mohr-Coulomb. Props (floor slabs) were modeled as fixed-end anchors.

The excavation by the top-down construction method proceeded from one side of the excavation to the other, with continuous casting of the floor slab. The 3D effects thus could not be neglected in the simulation (neither wished-in-place bracing nor bracing installation after excavation are relevant in the present case). To account for the 3D effects, the load-reduction method, often used in 2D simulations of NATM tunnels, has been used. Using this method, each excavation phase is sub-divided into two sub-phases. In the first one, the soil is excavated without a support. The support is installed after the first sub-phase, and the second sub-phase is simulated with the support active. The relative proportion of the two phases is quantified by the parameter β.

Obviously, β is merely an empirical parameter, and its value cannot be rigorously evaluated using the present data. For this reason, all simulations were run with different β factors, and the results were compared in a qualitative, rather then quantitative way.

7.1 Simulation results

Field measurements at the site included only inclinometer measurements of the horizontal displacements within the diaphragm walls. The measurements, altogether with simulations with different factors β are shown in Fig. 9. Figure 10 shows deformed meshes for the simulations with the two constitutive models.

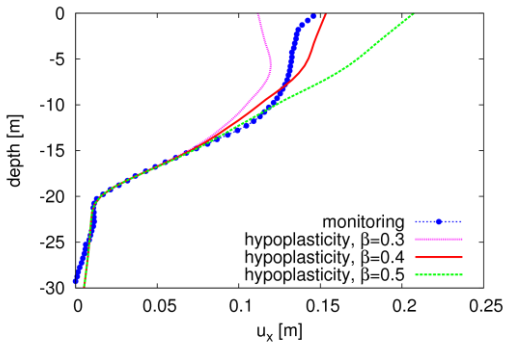

(a)

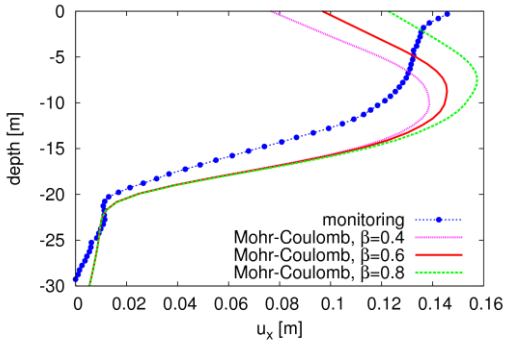

(b)

Figure 9. Comparison of inclinometric measurements of the diaphragm wall with simulation results. (a) hypoplasticity, (b) Mohr-Coulomb.

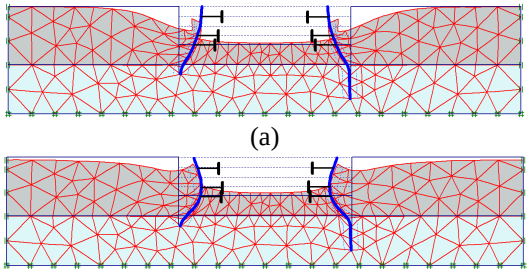

(a)

(b)

Figure 10. Deformed meshes (deformations not to scale) after the excavation construction. (a) hypoplasticity, (b) Mohr-Coulomb.

The results show that hypoplasticity and Mohr-Coulomb models lead to qualitatively different predictions, irrespective of the β factors used. Hypoplasticity predicts the largest horizontal displacements at the top of the diaphragm wall and the displacements gradually diminish towards the bottom. On the other hand, the Mohr-Coulomb model predicts the largest displacements in approximately one half of the excavation depth and a pronounced bulging of the walls. The field measurements agree qualitatively, and for β=0.4 also quantitatively, with the hypoplasticity predictions.

The difference is caused by the inability of the Mohr-Coulomb model to predict stress level and strain level and direction dependency of soil stiffness. These aspects of soil behavior are correctly incorporated within the hypoplastic model.

8 CONCLUSIONS

A case study of a deep excavation in soft silty clay has been described. Based on the experimental data, two constitutive models were calibrated – hypoplastic model with the intergranular strain concept and Mohr-Coulomb model. The hypoplastic model, thanks to the correct predictions of the state-dependent soil stiffness, gave predictions consistent with monitoring results. The Mohr-Coulomb model predicted incorrectly the deformation patter of the diaphragm walls.

ACKNOWLEDGEMENT

The financial support by the research grants of the Czech Science Foundation GACR P105/11/1884 and GACR 103/09/1262, and MSM 0021620855 is gratefully acknowledged.

REFERENCES

[1] Logar, J. Geotechnika v Luki Koper na začetku 21. stoletja. MS, Univerza v Ljubljani, Fakulteta za gradbeništvo in geodezijo. (2009).

[2] Mašín, D. A hypoplastic constitutive model for clays. *International Journal for Numerical and Analytical Methods in Geomechanics* **29** (2005), No. 4, 311-336

[3] Mašín, D. A hypoplastic constitutive model for clays with meta-stable structure. *Canadian Geotechnical Journal* **44** (2007), No. 3, 363-375.

[4] Niemunis, A. and Herle, I. Hypoplastic model for cohesionless soils with elastic strain range. *Mechanics of Cohesive-Frictional Materials* **2** (1997), 279–299.